ORIGINAL RESEARCH

The Mechanism of Catalpol to Improve Oxidative Damage of Dermal Fibroblasts Based on Nrf2/HO-1 Signaling Pathway

Xiaona Lang [1], Liyan Xu[2], Lu Li[1], Xin Feng[1]

[1]Pharmacy Department, Tianjin Hospital, Tianjin, People's Republic of China; [2]Orthopedic Department, Tianjin Hospital, Tianjin, People's Republic of China

Correspondence: Xin Feng, Pharmacy Department, Tianjin Hospital, Tianjin, People's Republic of China, Tel +86-13652001152, Email fx_yutong@126.com

Objective: Catalpol, as a natural medicine small-molecule drug, has been proven to have anti-inflammatory and antioxidant pharmacological effects.

Methods: The effect of catalpol on oxidative damage of mouse epidermal fibroblast L929 model and its mechanism were investigated by using hydrogen peroxide model, CCK8 method, flow cytometry, and Western blot.

Results: The effect of catalpol on Nrf2/HO-1 signaling pathway was further studied to improve oxidative stress in cell models. The results showed that catalpol had no cytotoxicity to L929 cells, and inhibited the apoptosis of L929 cells after oxidative damage in a concentration-dependent manner, thus playing a role in cell protection. The oxidative damage of cells was inhibited by up-regulating the expression of the signature protein of Nrf2/HO-1 signaling pathway and inhibiting the interstitial formation of cells.

Conclusion: This study is a preliminary study on the protective function of catalpol against oxidation and apoptosis in dermal fibroblasts, which can provide a theoretical basis and drug guidance for promoting skin wound healing in the later stage.

Keywords: catalpol, oxidative damage, Nrf2/HO-1, dermal fibroblasts, oxidative stress

Introduction

Dermal fibroblasts are the key cells in the wound healing process. When the skin is injured, the corium initiates an inflammatory response to clear tissue and pathogens from the damaged site. Dermal fibroblasts participate in the inflammatory process by releasing cytokines. These cytokines help attract more immune cells to the wound site and stimulate them to release more inflammatory substances in response to injury and infection.[1–4]

A close relationship exists between the inflammatory response of skin wounds and oxidative stress (OS). During the inflammatory process caused by trauma, cells release reactive oxygen species (ROS), increasing oxidative stress. Under normal circumstances, the ROS production and clearance system in the body is in a state of dynamic balance.[3,5] When the body is in the OS state, the ROS content in tissues and cells in the body is relatively increased, exceeding the body's scavenging ability, which can lead to the increase in lipid peroxidation level in tissues, resulting in oxidative damage of DNA and abnormal expression of protein, causing damage to the body.[6,7] Therefore, ROS levels are often used to assess the occurrence of OS.

Catalpol is a traditional Chinese medicine component of iridoid, widely existing in many Chinese medicine components, and can play a therapeutic role in many organs in the body.[8] Recent studies have proven that it has multiple pharmacological effects such as antioxidant, anti-inflammatory, anti-tumor, neuroprotective, hypoglycemic, etc.[9,10] In recent years, many studies have focused on the mechanism of catalpol's hypoglycemic and anti-tumor actions in vivo and in vitro.[9,11,12] However, the intervention's effect on dermal fibroblasts' function is still unclear. Through these experiments, we hope to know whether catalpol can also regulate the oxidative damage of dermal fibroblasts. This could expand the number of cell types catalpol regulates and explore its mechanisms of action in different cells.

Nrf2/HO-1 signaling pathway plays a key role in regulating oxidative stress response, and it has been confirmed that this pathway plays a significant role in oxidative stress.[13] As an antioxidant enzyme, Heme Oxygenase-1 (HO-1) has anti-inflammatory, antioxidant, and anti-proliferative effects when stimulating oxidative stress in the body, and is involved in the body's compensatory mechanism for oxidative stress, hypertension, and vascular reconstruction.[14] Nuclear Factor E2-associated Factor 2 (Nrf2) is inhibited in the cytoplasm and is rapidly degraded by the ubiquitin proteasome pathway.[15] When stimulated by oxidative stress signals, Nrf2 rapidly decouples with allosteric Kelch-like ECH Associated Protein 1 (Keap1), translocation into the nucleus to form a heterodimer in a stable state. Then, it binds to the gene's antioxidant response element (ARE). The expression of target genes mediated by ARE is increased to regulate the transcription and translation of antioxidant genes.[16,17]

This experiment first studied whether catalpol affected the oxidation-damaged mouse epidermal fibroblast L929 model and its mechanism of action.[18,19] In addition, we further investigated whether catalpol is involved in the Nrf2/HO-1 signaling pathway to affect oxidative stress in cell models.[20] Our study provides new insights into the mechanism of catalpol in oxidation-damaged dermal fibroblasts and valuable data and experience for our team's subsequent in vivo experiments.[21,22] Figure 1 shows the preliminary thinking and experimental prediction of this study.

Materials and Methods
Cell Culture
Mouse dermal fibroblasts L929 (Starfish Biology, TCM-C749) were taken from L929 cells at the logarithmic growth stage and supplemented with 1% penicillin and streptomycin mixture in DMEM/F12 (Corning, 10-092-CVRC) medium containing 10% fetal bovine serum (Soleboll, P1400). Penicillin (10kU/mL) and streptomycin (10mg/mL) in the stock solution were cultured at 37°C and 5% CO_2 in a constant temperature incubator.
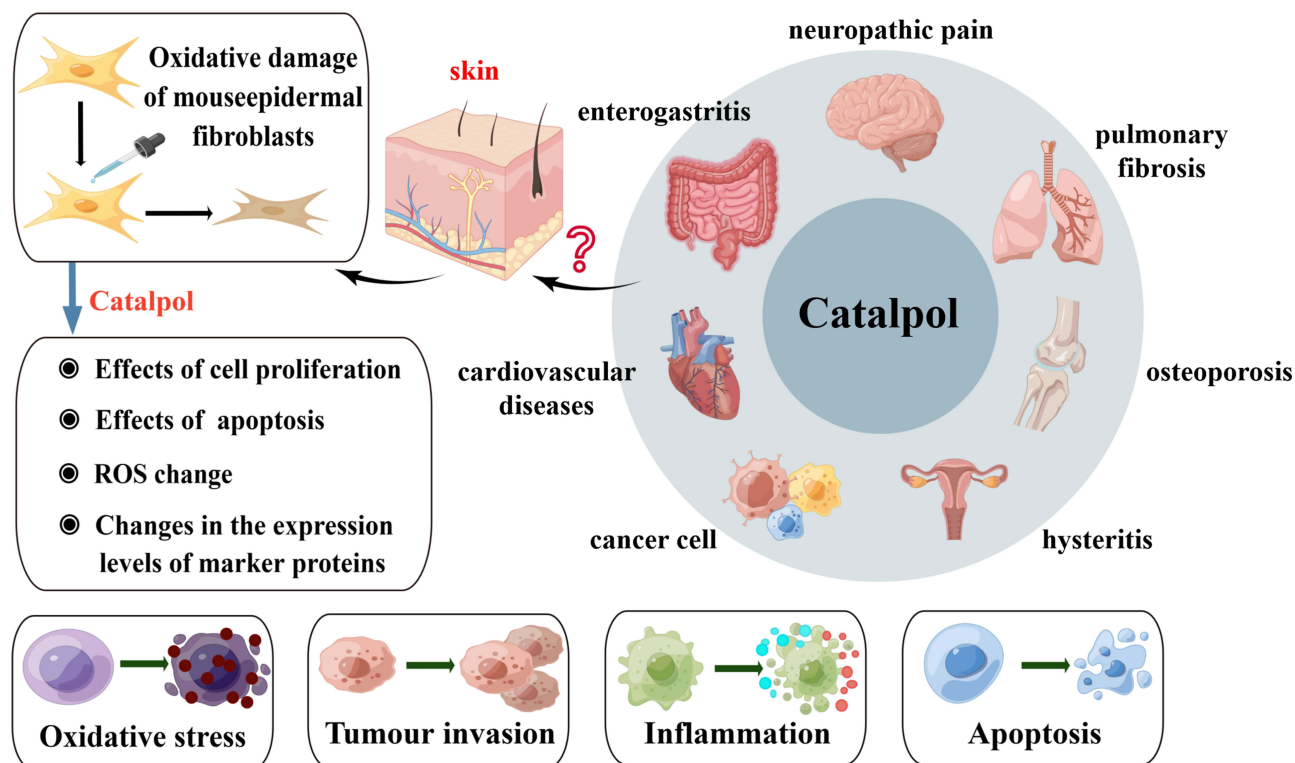

Figure 1 The proven mechanism of action of catalpol and the proposed experiment. (By Figdraw).

Materials and Reagents

Catalpol (CAT) (Aladdin, C110215, China), Hydrogen peroxide (H_2O_2) (Tianjin Damao Chemical Reagent Factory, analytical pure, China), N-acetylcysteine (NAC) (Aladdin, N170064, China), CCK8 (MCE, HY-K0301, NJ, USA), Medium (Corning, 10–092-CVRC, NY, USA), Fetal bovine serum (ExCell Bio, FSP500, China), 0.25% pancreatic enzyme (Gibco, 25200-072, CA, USA), Annexin V-FITC apoptosis detection kit (Beyotime Biotechnology, C1062L, China), Reactive oxygen species detection kit (Beyotime Biotechnology, S0033M, China), RIPA Lysis Solution (Beyotime Biotechnology, P0013, China), 5×loading buffer (Kang Weishi, CW0027S, China), PAGE Gel rapid preparation kit (Yi Sheng 10%: 20325ES, Yi Sheng 15%: 20327ES, China), Nrf2 antibody (Proteintech, lot No. 16396-1-AP, China), HO-1 antibody (Proteintech, Lot No. 16396-1-AP, Batch No. 10701-1-AP, China), Fibroblast-specific protein 1 (S100A4) antibody (Proteintech, Batch No. 16105-1-AP, China), fibroblast marker protein: Anti-smooth muscle antibody (alpha-SMA) antibody (Proteintech, batch No. 14395-1-AP, China).

Instruments

Enzymoscope, VICTOR NivoTM, PerkinElmer Corporation, USA. Flow cytometry, BD FACS CantoII, USA.

The Effect of Catalpol on Cells Was Detected

L929 cells at logarithmic growth stage were washed with PBS and collected after trypsinization at 37°C for 2 min. Then, L929 cells were centrifuged at 200 g for 5 min and resuspend with fresh medium. Thereafter, the cells were inoculated into 96-well plates at 5×10^3/ well and cultured overnight at 37°C and 5% CO_2. The experimental groups treated with different concentrations of catalpol were added (catalpol concentration was 2, 5, 10, 50, 100 μM, respectively) and continued to culture and treat at 5% CO_2 and 37°C for 24 hours. After 24 hours, CCK8 was added to detect cell viability in each group. Each group is provided with six multiple holes. Cell relative survival rate = (experimental group OD value − blank group OD value)/(regular control group OD value − empty group OD value). Each experiment was repeated three times.

Establishment of Oxidative Damage Model of Fibroblasts

L929 cells in the logarithmic growth phase were seeded at a density of 5×10^3 cells per well in 96-well plates and incubated overnight at 37°C with 5% CO_2. At the second day, the cells were treated with varying concentrations of H_2O_2 (50, 100, 200, 400, 600, 800, and 1000 μM) for 2 hours. The complete culture medium was used as the control group. After 2 hours, the H_2O_2-containing medium was replaced with fresh complete medium and incubated for an additional 24 hours. After 24 hours, CCK8 was performed to assess cell activity. The % relative survival rates of cells were plotted against concentrations of H_2O_2 and IC_{50} was calculated from the graph. Finally, according to the IC_{50}, the optimal induced concentration of the oxidative damage model was determined. Each group is provided with six multiple holes. Each experiment was repeated three times.

Detect the Effect of Catalpol on Cell Viability

L929 cells were seeded into 96-well plate at a density of 5×10^3 cells/200 μL/well and cultured overnight. L929 cells were treated with different concentrations of catapol (2 μM, 5 μM, 10 μM, 50 μM, and 100 μM), and the positive control NAC (500 μM). After 24 hours incubated, 400 μM H_2O_2 was added to each well for a 2 hours co-incubation at 37°C. Thereafter, the supernatant was discarded and replaced with a fresh complete culture medium cultured for 24 hours, 48 hours, and 72 hours, respectively. At different time points, the cells were incubated with 10% CCK8 solution for cell viability assay. The OD of each well at 450 nm was detected by a microplate reader after the 2 hours reaction. Each group was set up with three multiple holes, and the experiment was repeated three times. Each experiment was repeated three times.

Detect the Effect of Catalpol on Cell Apoptosis

Grouping and treatment were the same as the Detect the Effect of Catalpol on Cell Viability. The adherent cells were washed with PBS, collected after trypsinization, and washed twice with PBS. Then, resuspend cells in 1× Binding Buffer at a concentration of 1×10^6 cells/mL and transfer 100 μL of the solution to the tube. Add 5μL Annexin V-FITC, mix gently, then add 10 μL propyl iodide stain, and mix gently. Incubate at room temperature (20–25°C) without light for 10–20 minutes and then place in an ice bath and test on the machine within 1 hour. Each experiment was repeated three times.

Detect the ROS Content of the Cells

Grouping and treatment were the same as the Detect the Effect of Catalpol on Cell Viability. The adherent cells were washed with PBS and collected after trypsinization and washed twice with PBS. Then, the cells were resuspended in serum-free medium, and 100 μL DCFH-DA (1:1000) was added and incubated at 37°C without light for 30 min. The mean DCFH-DA was measured by flow cytometric analysis. Each experiment was repeated three times.

Determination of SOD, MDA, and GSH Activity

Group and drug intervention followed the same procedures outlined in the section Establishment of Oxidative Damage Model of Fibroblasts. After 24 hours, except for the blank control, each group was treated with H_2O_2 for 2 hours, and the H_2O_2 culture medium was removed and replaced with a complete medium for continuous culture for 24 hours. After 24 hours, L929 cells were broken up by ultrasound treatment and subjected to centrifugation by 8000g for 10 min. The SOD kit (Solarbio, #BC0025), MDA kit (solarbio, #BC0175), and GSH kit (Beytime, #S0053) were used, respectively, for the detections. Different OD values (560 nm for SOD, 532 nm for MDA, and 412 nm for GSH) were measured by a microplate reader. The activity of SOD, MDA, and GSH in each group was calculated according to the kit instructions.

Determination of the Expression Levels of Fibroblast Marker Proteins and Nrf2/HO-1 Signaling Pathway Marker Proteins

Grouping and drug intervention followed the same procedures outlined in the section Detect the Effect of Catalpol on Cell Viability. The total protein was extracted by discarding the supernatant medium and adding protein extraction reagents containing protease and phosphatase inhibitors. A BCA protein kit was used to detect total protein concentration. After 20 μg protein denaturation, the sample was transferred to 0.2 μm PVDF membrane by 10% SDS-PAGE gel electrophoresis, 260 mA, 1 h wet transfer, and sealed with 1×TBST containing skim milk powder /BSA according to the instructions of the primary antibody. The primary antibody (Nrf2, HO-1, S100A4, and α-SMA diluted at 1:1000 and β-actin diluted at 1:500) was added. The film was incubated overnight on a shaking bed at 4°C, washed four times with 1×TBST for 10 min each, and then incubated with a secondary antibody diluted at a ratio of 1:3000 for 1 hour. Following this, the film underwent three washes with 1×TBST for 10 min each, and the image was developed by chemiluminescence gel imager. Each group was set up with three multiple holes, and the experiment was repeated three times. β-actin was the internal reference protein, and Image J was used for gray analysis of the bands. Each experiment was repeated three times.

Statistical Analysis

FlowJo 7.6.1 software for flow analysis. GraphPad Prism 8.0 software plotted each experimental data, and all data were expressed as mean ± standard deviation ($\bar{x} \pm s$). IBM SPSS 23 software was used for statistical analysis of experimental data and one-way AVONA compared differences between groups. The Kolmogorov–Smirnov (K-S) test was used to test the normality of the data, and the F-test for the homogeneity of the variance. Fisher's LSD test was used for planned post-hoc pairwise comparisons. $p < 0.05$ indicates a statistically significant difference.

Results and Discussion

Toxicity of Catalpol to L929 Cells

Compared with the regular group, different concentrations of catalpol treated normal L929 cells for 24 hours, and the decreasing trend of cell viability was not noticeable. Cell viability was slightly decreased in the 100 μmol·L^{-1} catalpol group (p < 0.05), and the lowest value in the six repeated experiments was also above 80%, as shown in Figure 2A.
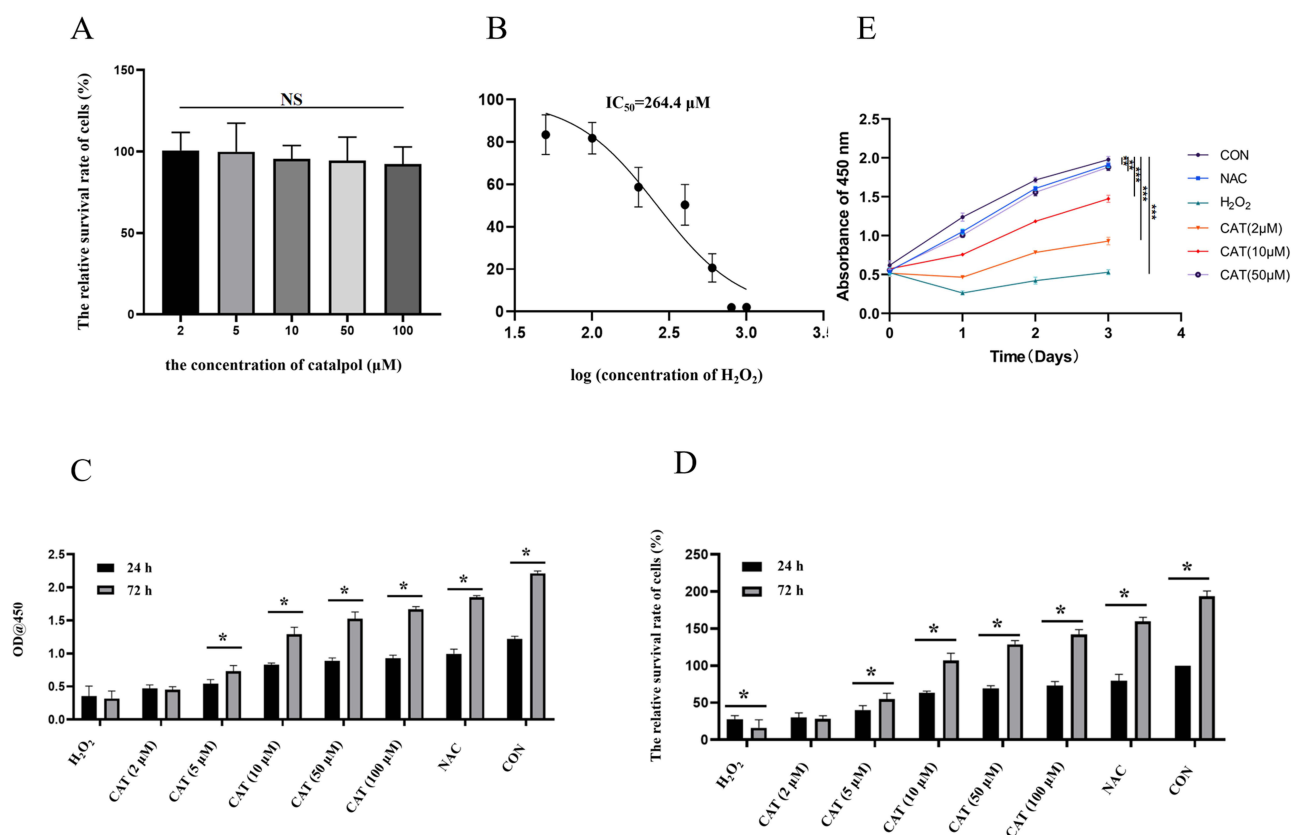
The Cell Model of H_2O_2-Induced Oxidative Damage Was Optimized

With the increase in H_2O_2 concentration and time, the activity of L929 cells decreased gradually. After 2-hour treatment with different concentrations of H_2O_2, the difference in H_2O_2 concentrations (50, 100, 200, 400, 600, 800, and 1000 μM) was statistically significant, and the IC$_{50}$ value was 264.4 μM. In order to prevent excessive oxidative damage to L929 cells, 400 μM was selected as the appropriate concentration for the oxidative damage cell model, as shown in Figure 2B.

Effect of Catalpol on Viability of Cell Model with Oxidative Damage

Compared with the negative control group, OD value and relative cell survival rate induced by H_2O_2 in the catalpol intervention group increased in a concentration-dependent way after incubation for 24 hours and 72 hours, and viability was significantly increased, as shown in Figure 2C and D.

Compared to the negative control group, the cells underwent ROS and apoptosis, so after 24 hours and 72 hours, the cell survival rate was lower than that of the standard control group. The relative survival rate of cells in different concentration groups of catalpol increased significantly (p < 0.05), suggesting that catalpol effectively protected L929 cells.

Figure 2 H_2O_2-induced oxidative damage cell model and effect of catalpol on viability of cell model with oxidative damage. (**A**) CCK8 assay for evaluating the effect of catalpol on L929 cell proliferation. (**B**) Assessment of oxidative damage on L929 cells with H_2O_2 treated. (**C**) CCK8 assay evaluating protective effects of catalpol on H_2O_2 treated L929 cells. (**D**) IC$_{50}$ values of H_2O_2 in L929 cells. Data are presented as the average of repeated samples, with error bars representing standard deviations. *p <0.05. (**E**) The cell proliferation ability of L929 cells which were pretreatment with NAC and different concentrations of catalpol in H_2O_2 induced oxidative stress model for 24 h, 48 h, 72 h.

Meanwhile, we evaluated the cell proliferation ability using CCK8 assay, As shown in Figure 2E, H_2O_2 inhibited the growth of L929 cells. The cell proliferation ability was significantly increased with NAC and different concentrations of catalpol.
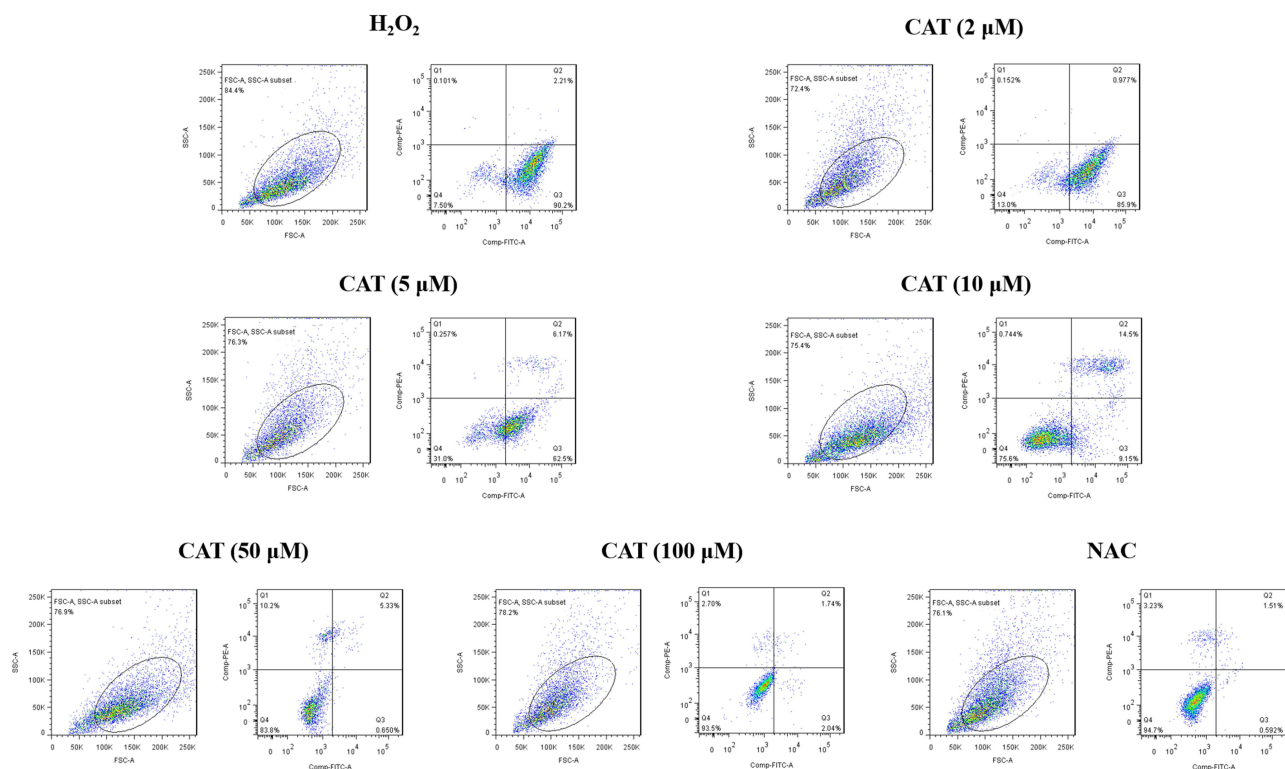
Effect of Catalpol on Apoptosis of Model Cells Damaged by Oxidation

Compared with the negative control group, the H_2O_2-induced apoptosis rate in the catalpol intervention group decreased in a concentration-dependent manner after incubation for 24 hours, and apoptosis was significantly inhibited. Twenty-four-hour flow cytometry showed that the apoptosis rates of negative control group, catalpol intervention group (2, 5, 10, 50, 100 μM) and positive control group were, respectively, 92.31%±1.12%; 86.39%±3.22%; 66.86%±1.81%; 26.01% ±2.32%; 5.68%±1.14%; 3.62%±0.79%; 2.91%±0.78%; 1.26%±0.12%. By Figure 3.

Compared with the negative control group, the apoptosis rate of catalpol in different concentration groups was significantly decreased ($p < 0.05$), suggesting that catalpol effectively protected L929 cells and prevented apoptosis induced by oxidative damage to a certain extent. Through the data analysis of 3.1–3.4, the appropriate concentration of catalpol in the next experiment was set as follows: 2, 10, and 50 μM.

Effects of Catalpol on ROS in L929 Cells Damaged by Oxidation

Compared with the blank control group, ROS content in the negative control group was increased ($p < 0.05$). Compared with the negative control group, ROS content in the catalpol group (2, 10, 50 μM) was dose-dependent decreased ($p < 0.05$), as shown in Figure 4A. When the concentration of catalpol reached 50 μM, its ROS content was similar to that of the NAC group, thereby reducing cellular oxidative damage, as shown in Figure 4B. Figure 4C shows the average fluorescence intensity of different experimental groups. The moderate fluorescence intensity is proportional to the ROS level, which can also reflect the changes in ROS level in other experimental groups.

Figure 3 Effect of catalpol on apoptosis of model cells damaged by oxidation. Flow cytometry for evaluating the effect of catalpol on apoptosis in H_2O_2 treated L929 cells.
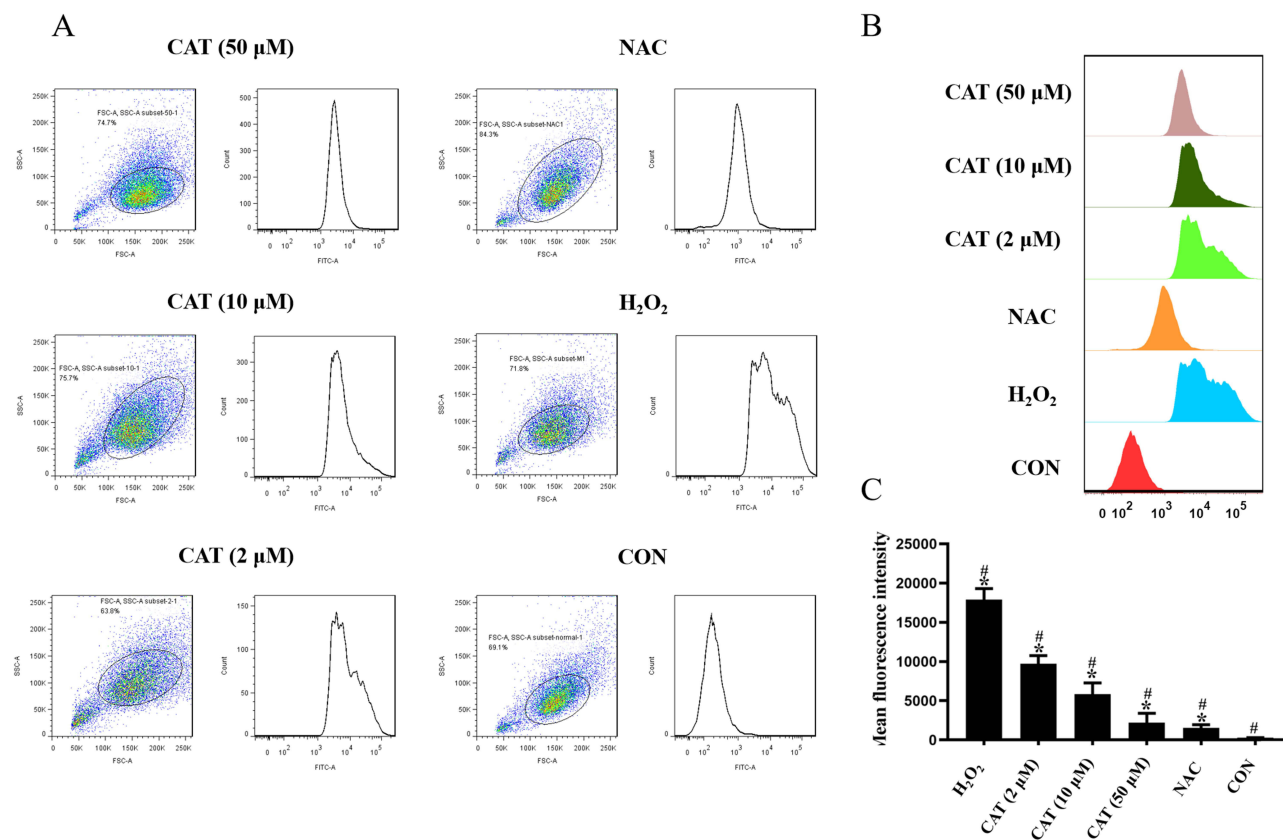
Figure 4 Effects of catalpol on ROS in L929 cells damaged by oxidation. (**A** and **B**) Flow cytometric analysis of the ROS production in L929 cells with different treatments. (**C**) Quantitative analysis of DCFH-DA accumulation by FACS. Data are presented as the average of repeated samples, with error bars representing standard deviations. *p <0.05, #p <0.05.

Effects of Catalpol on H_2O_2-Induced Oxidative Injury in L929 Cells

To examine the effects of catalpol on oxidative stress, we measured the level of SOD, GSH, and MDA. As shown in Figure 5A and B, the levels of SOD and GSH were significantly reduced in H_2O_2-treated L929 cells, but catalpol significantly restored the levels of SOD and GSH dose-dependently. H_2O_2 leads to the production of ROS and subsequently causes lipid peroxidation of the biomembrane, which leads to the production of a large amount of MDA. Therefore, we measured the levels of MDA in H_2O_2-treated L929 cells. As shown in Figure 5C, the levels of MDA were significantly elevated with H_2O_2 treated, whereas decreased in L929 cells pretreated with catalpol. Therefore, catalpol could enhance antioxidant cap**acity.**
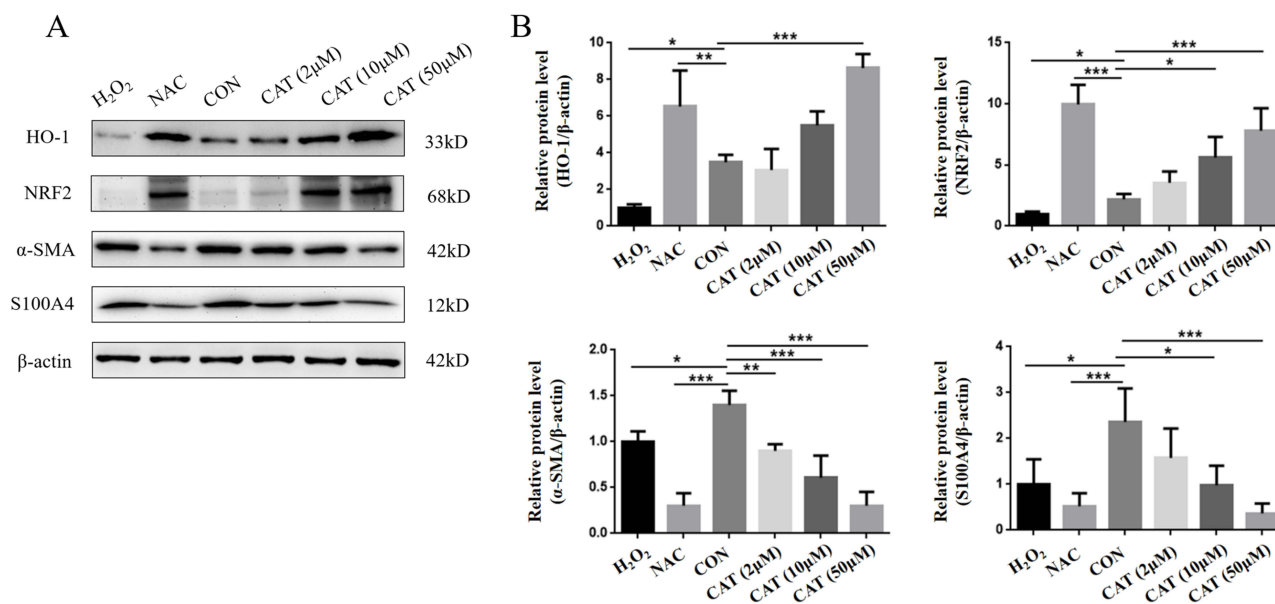
Effects of Catalpol on Oxidative Damage of L929 Cell Marker Protein and Nrf2/HO-1 Pathway Protein

Nrf2 and HO-1 are antioxidant stress-related proteins that play a protective role in cells. We assessed the effects of catalpol on the Nrf2/HO-1 pathway. As shown in Figure 6A and B, the level of Nrf2 and HO-1 was decreased in H_2O_2-treated L929 cells. Pretreatment with N-acetyl cysteine (NAC), a free radical scavenger, reversed the H_2O_2-induced Nrf2/HO-1 down-regulation. Meanwhile, catalpol increased their levels in a dose–effect manner. Thus, Nrf2/HO-1 pathway may be activated by catalpol in L929 cells.

α-SMA and S100A4 are important markers for fibroblasts. In this study, we investigated the effect of Catalpol on α-SMA and S100A4. As shown in Figure 6A, H_2O_2 decreased fibroblast marker expression with oxidative damage. Oxidative stress is an important factor in activating EMT. Both α-SMA and S100A4 are also epithelial and mesenchymal markers. And considering the antitumor properties of catalpol, L929 cells altered their mesenchymal phenotypes with catalpol treatment. As shown in Figure 6A and B, the expressions of α-SMA and S100A4 were reversed in L929 cells pretreated with catalpol. Our result indicated that catalpol altered mesenchymal phenotypes of L929 cells induced by H_2O_2.
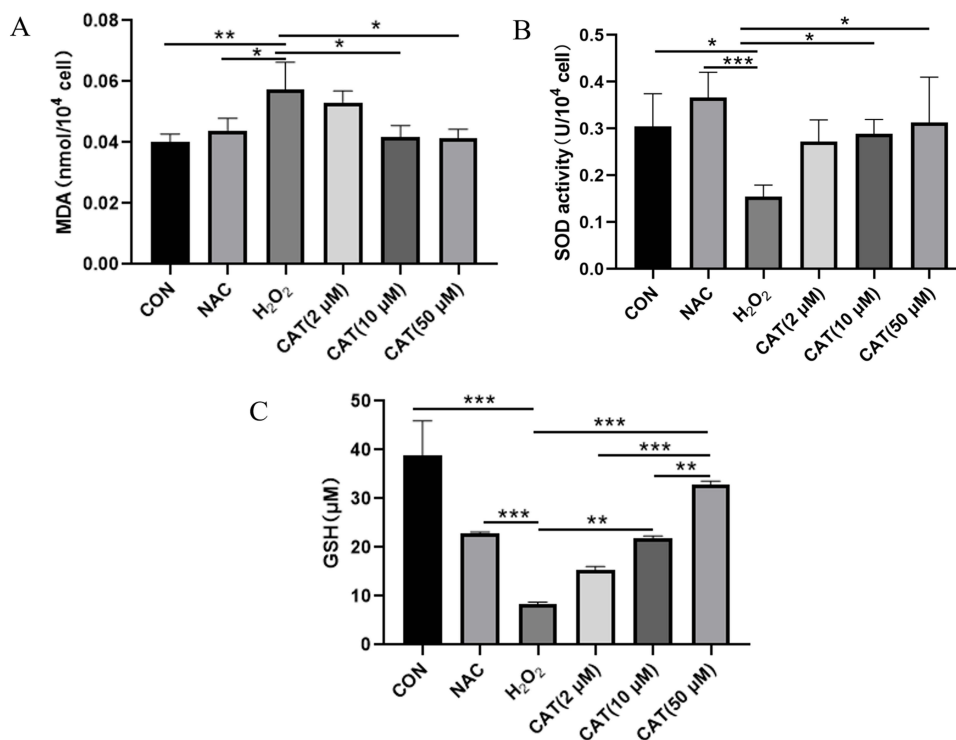
Figure 5 (**A**) Effects of catalpol on MDA in L929 cells damaged by oxidation. (**B**) Effects of catalpol on SOD in L929 cells damaged by oxidation. (**C**) Effects of catalpol on GSH in L929 cells damaged by oxidation. *p <0.05, **p <0.01, ***p <0.001.

Figure 6 Effects of catalpol on oxidative damage of L929 cell marker protein and Nrf2/HO-1 pathway protein. (**A**) Western blot analyzed Nrf2, HO-1, α-SMA and S100A4 expression in H_2O_2-treated L929 cells which were pretreatment with NAC and different concentrations of catalpol for 24 hours. (**B**) Statistical analysis of Nrf2, HO-1, α-SMA and S100A4 expression in H_2O_2-treated L929 cells which were pretreatment with NAC and different concentrations of catalpol for 24 hours. Data are presented as the average of repeated samples, with error bars representing standard deviations. *p <0.05, **p <0.01, ***p <0.001.

Discussion

The results showed that pretreatment with catalpol significantly increased cell viability and reduced apoptosis in H_2O_2-treated L929 cells. Catalpol also effectively reduced the production of ROS and free radicals in the cells, indicating its antioxidant

properties. Furthermore, catalpol was found to upregulate the expression of antioxidant enzymes such as superoxide dismutase (SOD) and glutathione peroxidase (GPx), which play a crucial role in protecting cells from oxidative damage. Overall, these findings suggest that catalpol exerts protective effects on L929 cells against H_2O_2-induced oxidative stress and apoptosis by enhancing antioxidant defense mechanisms. Therefore, catalpol may have potential therapeutic applications in conditions involving oxidative stress and cell damage. Further research is needed to elucidate the underlying molecular mechanisms of catalpol's protective effects and explore its potential clinical applications.[23,24]

The pharmacodynamic experiment of catalpol showed that different concentrations of catalpol (2–100 μM) had no inhibitory effect on the viability of normal L929 cells. According to the analysis of CCK8 and flow cytometry results, catalpol 2, 10, 50 μM were selected as the appropriate dosage concentrations for follow-up experiments. The results of this study showed that catalpol alleviated the inhibition of Nrf2 and up-regulated HO-1 expression, as shown in Figure 7A. Figure 7B briefly describes the process of oxidative stress. Figure 7C depicts the Nrf2/HO-1 signaling pathway. The conclusion is that catalpol can reduce the damage caused by oxidative stress by up-regulating the protein expression of Nrf2/HO-1 signaling pathway. Catalpol and NAC can clear ROS and reduce cell damage caused by ROS.[25–27] Catalpol and NAC can protect cells from apoptosis but cannot promote cell viability after treatment. In the previous CCK8 experiment, it was only found that catalpol or NAC-treated cells had no effect on cell viability, while hydrogen-peroxide-treated cells generated ROS and apoptosis, so the cell survival rate was lower than that of the standard control group after 24 hours and 72 hours.

So far, the published studies on catalpol are about its mechanism of action on tumor cells, islet cells, and so on. There is no cell research on the skin yet. Therefore, these experiments are to fill the gap in this aspect.
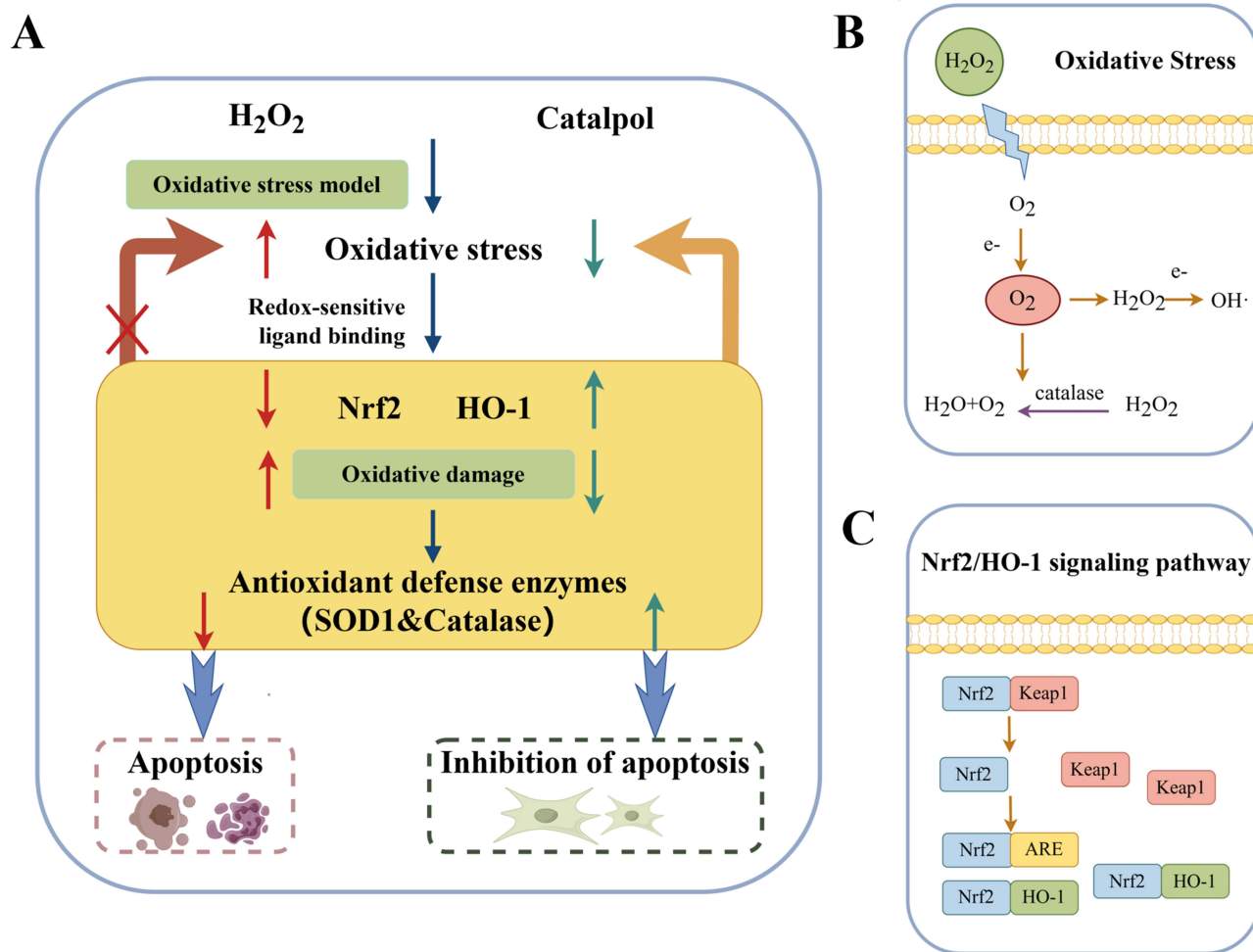
Figure 7 (**A**) Mechanism diagram of catalpol obtained by experiment; (**B**) Relationship between OS and H_2O_2. (**C**) Schematic diagram of Nrf2/HO-1 signaling pathway.

Conclusion

Catalpol, a new terpenoid hypoglycemic active monomer type, was approved for clinical trials of a new class of traditional Chinese medicine in China in 2017.[28] Because it is one of the newly discovered small-molecule drugs, there are still few studies related to catalpol, which can bring us not too much enlightenment. Fortunately, more and more researchers have begun to pay attention to monomer drugs and are keen to use them in the clinic. This is an increasingly clear development for Chinese medicine in the field of medical research around the world. Although the bioavailability of catalpol is low, part of its activity and mechanism of action has been determined, and the optimization of the structure or the use of nano preparation technology is expected to develop drugs to promote skin wound healing in the future. Therefore, it is essential to strengthen the basic research on the antioxidant mechanism of catalpol on fibroblasts.[29–34] Before the experiment began, the research group had predicted the correlation between catalpol and the functional targets of L929 cells by molecular docking simulation and speculated that catalpol could reduce the apoptosis induced by excessive oxidative stress and improve the function of L929 cells. This study is a preliminary study on the protective function of catalpol against oxidation and apoptosis in dermal fibroblasts, which can provide a theoretical basis and drug guidance for promoting skin wound healing at a later stage.

Data Sharing Statement

All the data in the article are obtained by the authors themselves, and the pictures are also drawn by themselves. So no reference to any data set, all original. Six samples were prepared for each data, and the repeated experiment of each sample was carried out as a separate and independent experiment.

Ethical Approval

No ethical approval is required for this article.

Author Contributions

All authors made a significant contribution to the work reported, whether that is in the conception, study design, execution, acquisition of data, analysis and interpretation, or in all these areas; took part in drafting, revising or critically reviewing the article; gave final approval of the version to be published; have agreed on the journal to which the article has been submitted; and agree to be accountable for all aspects of the work.

Funding

Disclosure

The authors declare that the research was conducted without any commercial or financial relationships construed as a potential conflict of interest.

References

1. Abbasi S, Sinha S, Labit E, et al. Distinct regulatory programs control the latent regenerative potential of dermal fibroblasts during wound healing. *Cell Stem Cell*. 2020;27(3):396–412 e6. doi:10.1016/j.stem.2020.07.008
2. Dekoninck S, Blanpain C. Stem cell dynamics, migration and plasticity during wound healing. *Nat Cell Biol*. 2019;21(1):18–24. doi:10.1038/s41556-018-0237-6
3. Dong S, Guo X, Han F, He Z, Wang Y. Emerging role of natural products in cancer immunotherapy. *Acta Pharm Sin B*. 2022;12(3):1163–1185. doi:10.1016/j.apsb.2021.08.020
4. Wu F, Yang J, Liu J, et al. Signaling pathways in cancer-associated fibroblasts and targeted therapy for cancer. *Signal Transduct Target Ther*. 2021;6(1):218. doi:10.1038/s41392-021-00641-0
5. Komi DEA, Khomtchouk K, Santa Maria PL. A review of the contribution of mast cells in wound healing: involved molecular and cellular mechanisms. *Clin Rev Allergy Immunol*. 2020;58(3):298–312. doi:10.1007/s12016-019-08729-w
6. Lin Y, Jiang M, Chen W, Zhao T, Wei Y. Cancer and ER stress: mutual crosstalk between autophagy, oxidative stress and inflammatory response. *Biomed Pharmacother*. 2019;118:109249. doi:10.1016/j.biopha.2019.109249
7. Sahoo DK, Heilmann RM, Paital B, et al. Oxidative stress, hormones, and effects of natural antioxidants on intestinal inflammation in inflammatory bowel disease. *Front Endocrinol*. 2023;14:1217165. doi:10.3389/fendo.2023.1217165

8. Hu H, Wang C, Jin Y, et al. Catalpol inhibits homocysteine-induced oxidation and inflammation via inhibiting Nox4/NF-kappaB and GRP78/PERK pathways in human aorta endothelial cells. *Inflammation*. 2019;42(1):64–80. doi:10.1007/s10753-018-0873-9

9. Bhattamisra SK, Koh HM, Lim SY, Choudhury H, Pandey M. Molecular and biochemical pathways of catalpol in alleviating diabetes mellitus and its complications. *Biomolecules*. 2021;11(2). doi:10.3390/biom11020323

10. Chen H, Deng C, Meng Z, Meng S. Effects of catalpol on Alzheimer's disease and its mechanisms. *Evid Based Complement Alternat Med*. 2022;2022:2794243. doi:10.1155/2022/2794243

11. Bai Y, Zhu R, Tian Y, et al. Catalpol in diabetes and its complications: a review of pharmacology, pharmacokinetics, and safety. *Molecules*. 2019;24 (18). doi:10.3390/molecules24183302

12. Qiao PF, Yao L, Zeng ZL. Catalpol-mediated microRNA-34a suppresses autophagy and malignancy by regulating SIRT1 in colorectal cancer. *Oncol Rep*. 2020;43(4):1053–1066. doi:10.3892/or.2020.7494

13. Li B, Nasser MI, Masood M, et al. Efficiency of Traditional Chinese medicine targeting the Nrf2/HO-1 signaling pathway. *Biomed Pharmacother*. 2020;126:110074. doi:10.1016/j.biopha.2020.110074

14. Ryter SW. Heme oxgenase-1, a cardinal modulator of regulated cell death and inflammation. *Cells*. 2021;10(3). doi:10.3390/cells10030515

15. He F, Ru X, Wen T. NRF2, a transcription factor for stress response and beyond. *Int J Mol Sci*. 2020;21(13). doi:10.3390/ijms21134777

16. Gao X, Hu W, Qian D, et al. The mechanisms of ferroptosis under hypoxia. *Cell Mol Neurobiol*. 2023;43(7):3329–3341. doi:10.1007/s10571-023-01388-8

17. Khoshandam A, Razavi BM, Hosseinzadeh H. Interaction of saffron and its constituents with Nrf2 signaling pathway: a review. *Iran J Basic Med Sci*. 2022;25(7):789–798. doi:10.22038/IJBMS.2022.61986.13719

18. Patil S, Licari FW, Bhandi S, et al. The cytotoxic effect of thermoplastic denture base resins: a systematic review. *J Funct Biomater*. 2023;14(8). doi:10.3390/jfb14080411

19. Peranidze K, Safronova TV, Kildeeva NR. Electrospun nanomaterials based on cellulose and its derivatives for cell cultures: recent developments and challenges. *Polymers*. 2023;15(5). doi:10.3390/polym15051174

20. Zhang Z, Dai Y, Xiao Y, Liu Q. Protective effects of catalpol on cardio-cerebrovascular diseases: a comprehensive review. *J Pharm Anal*. 2023;13 (10):1089–1101. doi:10.1016/j.jpha.2023.06.010

21. Bhattamisra SK, Yap KH, Rao V, Choudhury H. Multiple biological effects of an iridoid glucoside, catalpol and its underlying molecular mechanisms. *Biomolecules*. 2019;10(1). doi:10.3390/biom10010032

22. Fu Z, Su X, Zhou Q, Feng H, Ding R, Ye H. Protective effects and possible mechanisms of catalpol against diabetic nephropathy in animal models: a systematic review and meta-analysis. *Front Pharmacol*. 2023;14:1192694. doi:10.3389/fphar.2023.1192694

23. He L, Zhao R, Wang Y, Liu H, Wang X. Research progress on catalpol as treatment for atherosclerosis. *Front Pharmacol*. 2021;12:716125. doi:10.3389/fphar.2021.716125

24. Zheng XW, Yang WT, Chen S, et al. Neuroprotection of catalpol for experimental acute focal ischemic stroke: preclinical evidence and possible mechanisms of antioxidation, anti-inflammation, and antiapoptosis. *Oxid Med Cell Longev*. 2017;2017:5058609. doi:10.1155/2017/5058609

25. Jia J, Chen J, Wang G, Li M, Zheng Q, Li D. Progress of research into the pharmacological effect and clinical application of the traditional Chinese medicine Rehmanniae Radix. *Biomed Pharmacother*. 2023;168:115809. doi:10.1016/j.biopha.2023.115809

26. Teschke R. Treatment of Drug-Induced Liver Injury. *Biomedicines*. 2022;11(1). doi:10.3390/biomedicines11010015

27. Yuan H, Yang M, Han X, Ni X. The therapeutic effect of the Chinese herbal medicine, rehmanniae radix preparata, in attention deficit hyperactivity disorder via reversal of structural abnormalities in the cortex. *Evid Based Complement Alternat Med*. 2018;2018:3052058. doi:10.1155/2018/3052058

28. Dinda B, Dinda M, Kulsi G, Chakraborty A, Dinda S. Therapeutic potentials of plant iridoids in Alzheimer's and Parkinson's diseases: a review. *Eur J Med Chem*. 2019;169:185–199. doi:10.1016/j.ejmech.2019.03.009

29. Bai R, Jie X, Yao C, Xie Y. Discovery of small-molecule candidates against inflammatory bowel disease. *Eur J Med Chem*. 2020;185:111805. doi:10.1016/j.ejmech.2019.111805

30. Kalkreuter E, Pan G, Cepeda AJ, Shen B. Targeting bacterial genomes for natural product discovery. *Trends Pharmacol Sci*. 2020;41(1):13–26. doi:10.1016/j.tips.2019.11.002

31. Liu Y, Yang S, Wang K, et al. Cellular senescence and cancer: focusing on traditional Chinese medicine and natural products. *Cell Prolif*. 2020;53 (10):e12894. doi:10.1111/cpr.12894

32. Nasim N, Sandeep IS, Mohanty S. Plant-derived natural products for drug discovery: current approaches and prospects. *Nucleus*. 2022;65 (3):399–411. doi:10.1007/s13237-022-00405-3

33. Yin B, Fang DM, Zhou XL, Gao F. Natural products as important tyrosine kinase inhibitors. *Eur J Med Chem*. 2019;182:111664. doi:10.1016/j.ejmech.2019.111664

34. Zheng W, Wu Y, Gao H, Ouyang D. Traditional Chinese medicine injections: where we are after 80-year development. *Chin Med*. 2022;17(1):127. doi:10.1186/s13020-022-00681-w